

# The electrodeposition of aluminium from xylene and ether-hydride electrolytes

S. BIALLOZOR\*, V. MAZIN†, M. LIEDER

Technical University of Gdansk, Faculty of Chemistry, Majakowskiego 11/12, 80–952 Gdansk, Poland

Received 3 January 1992; revised 7 July 1992

A comparative study of aluminium electrodeposition from xylene and ether electrolytes is presented. The kinetic parameters of aluminium deposition from the tetrahydrofuran (THF) and xylene electrolytes are presented. In the case of the THF and diethylether solutions investigations of aluminium nucleation were also made. It was found that the rate of aluminium deposition was highest in the THF electrolyte composed of  $\text{AlCl}_3$  and  $\text{LiAlH}_4$  in a ratio 1:1. This electrolyte is recommended for deposition of aluminium protective coatings of thickness over  $20\ \mu\text{m}$

## 1. Introduction

There are three types of prospective electrolytes for electrodeposition of aluminium: alkylaluminium (Sigal process), ether-hydride (NBS bath and REAL process) and alkylbenzene. At present only the Sigal process is used in practice. However, xylene and ether hydride electrolytes are possibly much more suitable for the following reasons: lower solution flammability and toxicity, ambient temperature electrolysis, simple methods of preparation and utilization. A review of organic electrolytes for aluminium electrodeposition has been published by Galova [1].

In Table 1 some new technological parameters for aluminium electrodeposition from various electrolytes are summarized. It must be noted, that the xylene electrolyte is very simple in terms of preparation and operation. However, it cannot be used for obtaining an aluminium layer thicker than  $20\ \mu\text{m}$ .

In this paper new data for electrodeposition of aluminium from xylene and ether-hydride electrolytes are presented.

## 2. Experimental details

The reagents and electrolytes were prepared by techniques described earlier [2,3]. All operations with the solutions were carried out in a dry glove box under an argon atmosphere. An undivided, three-electrode electrolysis cell was used in all experiments. An aluminium rod (99.9% purity) was used as anode. An aluminium wire served as a reference electrode and all potentials given in the paper refer to this electrode. The working electrode was a platinum wire sealed in a glass tube. The surface of the platinum cathode was polished with emery paper of 800–1000 grades, cleaned in concentrated  $\text{H}_2\text{SO}_4$ , rinsed in redistilled water and acetone and then dried carefully.

Cyclic voltammetry (CV), chronoamperometry (CA) and impedance spectra measurements were applied. The measurements were carried out at 298 K.

## 3. Results and discussion

Figure 1 shows typical cyclic voltammetric curves (CV) obtained in diethylether (DEE) and tetrahydrofuran (THF) electrolytes. The cathodic branch of the CV curve for the THF solution comprises three waves. Furthermore, the current efficiency of aluminium deposition at currents not exceeding the third wave is 100%. These facts indicate the participation of three different aluminium complexes in the electro-reduction process. This has been discussed, in detail, in [7].

The main characteristic data for the ether electrolytes obtained by CV are shown in Table 2. It can be seen that the data for the THF solutions containing  $\text{AlCl}_3$  and  $\text{LiAlH}_4$  in a ratio 1:3 and 1:1 are comparable, although the rate of the cathodic process in the latter solution is higher. This conclusion can be drawn from comparison of the anodic peak currents ( $j_{pa}$ ) and the charge consumed during anodic dissolution ( $Q_a$ ) for these electrolytes. The cathodic process proceeds with higher overpotential and at a lower rate in the 3:1 electrolyte. Further studies were confined to the THF electrolytes because  $j_{pa}$  dramatically decreases in the DEE electrolyte (Fig. 1b).

In Table 2 some characteristics of CV curves obtained for the xylene electrolytes are also shown. Nucleation potentials ( $E_n$ ) in this solution are distinctly more positive, so coarse grains are likely to be deposited due to the lower overpotential.

The coefficients  $a_{c,a}n$  calculated from a Tafel equation for the backward branches of the CV curves ( $v = 0.01\ \text{V s}^{-1}$ ) are shown in Table 3. A relation  $a_c + a_a = 1$  is fulfilled for the xylene electrolytes,

\* To whom all correspondence should be sent.

† On leave from Institute of Physical Chemistry, Russian Academy of Sciences, Moscow, Russia.

Table 1. Technological parameters for aluminium electrodeposition from some organic solutions

Solvent	Main components	Parameters					Ref.
		$10^3 \times j_{\text{max}} / \text{Sm cm}^{-1}$	Temp. / °C	$j_{\text{max}} / \text{A m}^{-2}$	$W_{\text{Al}} / \%$	Deposit quality	
Toluene	$\text{Al}(\text{C}_2\text{H}_5)_3$ NaF	9	80–100	1–2	100	fine	[4]
Xylene	$\text{AlBr}_3$	8.8	20–40	$\leq 1$	90–95	coarse	[3]
THF	$\text{AlCl}_3$	8–10	20–40	1–5	100	fine	[2]
THF 55% vol	$\text{LiAlH}_4$						
Benzene 45% vol	$\text{AlCl}_3$	6–8	20–30	1–3	100	fine	[5]
THF 70% vol	$\text{LiAlH}_4$	7–10	20–40	1–8	100	fine	[6]
Octane 30% vol	$\text{LiAlH}_4$						

whereas  $a_c + a_a < 1$  (when  $n = 3$ ) for the THF solutions. Similar results were obtained by Kazakov *et al* [8].

The number of electrons,  $n$ , transferred in the slowest step of the reaction may vary depending on solution type or the experiment procedure. To date there is no consensus on the number of electrons taking part in the rate determining step of the cathodic deposition

of aluminium. Some authors established  $n = 3$ , while others obtained  $n = 1$  [9]. The present results indicate that  $n = 3$  for the THF solutions, whereas for the aromatic electrolytes  $n = 1$ . The solvent appears to determine the controlling step of the cathodic charge transfer.

The solutions containing higher concentrations of  $\text{LiAlH}_4$  (for example  $\text{AlCl}_3 : \text{LiAlH}_4 = 1 : 3$ ) are very unstable due to polymerization. For this reason, these solutions cannot find application in practice and, therefore, it was decided to confine further studies to the electrolytes composed of  $\text{AlCl}_3$  and  $\text{LiAlH}_4$  in a concentration ratio of 1 : 1 or 3 : 1.

In Figs 2 and 3 the Nyquist plots are shown. Their shapes for the THF electrolytes indicate an electrode process which consists of a number of parallel reactions [10], which confirms the assumption that various aluminium complexes take part in the electrode reactions. However, these results are not consistent with the mechanism proposed by Galova *et al.* [11]. The impedance spectra for the xylene electrolytes indicate diffusion control of the deposition, provided that the overpotential is higher than 0.3 V. It has been shown [12] that Al deposition in aromatic electrolytes proceeds along with a thin layer formation, being a product of the solvent polymerization. This leads to the partial blocking of the electrode active sites resulting in a current efficiency drop.

In Fig. 4 typical CA curves obtained for the THF and xylene electrolytes are shown. There is a maximum in the  $J-t$  curves for THF solutions and the calculation procedure recommended by Scharifker can be adopted

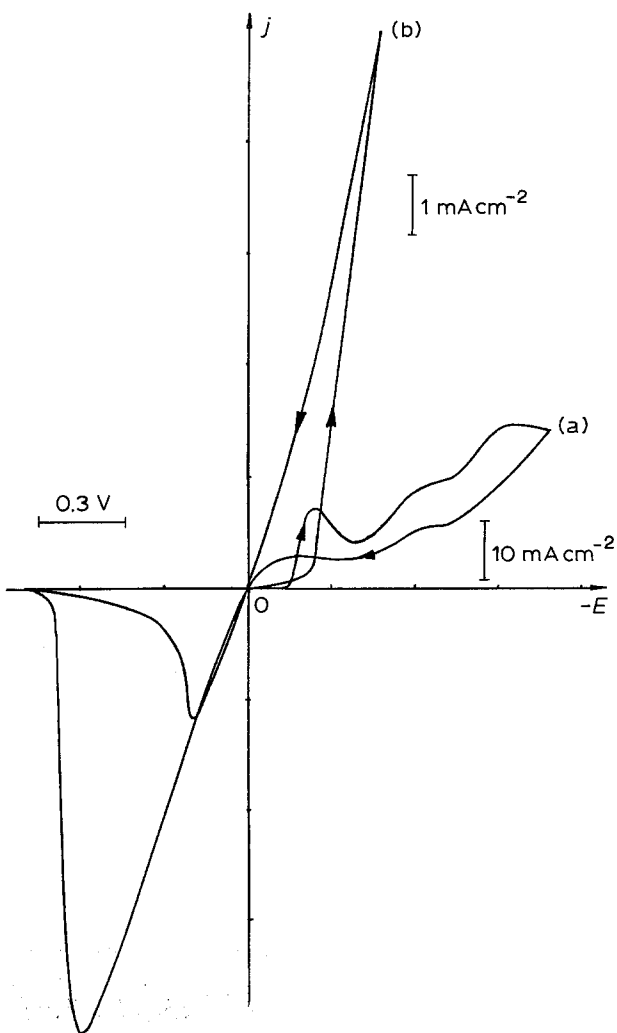


Fig. 1. Typical voltammetric curves recorded in the (a) THF and (b) DEE solutions, where  $\text{Al}_{\text{total}} = 0.5 \text{ M}$  and a ratio  $\text{AlCl}_3 : \text{LiAlH}_4 = 3$ . Scan rate  $v = 0.1 \text{ V s}^{-1}$ .

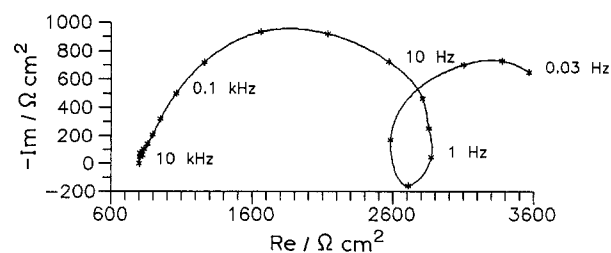
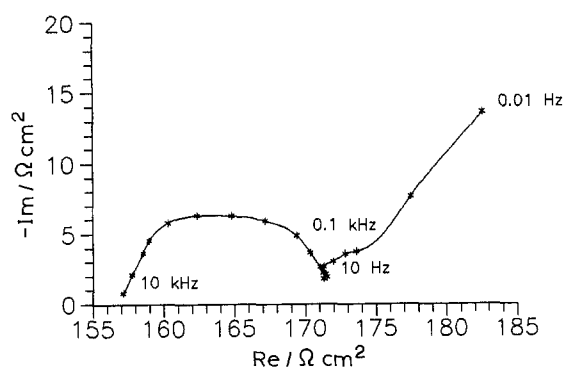


Fig. 2. A Nyquist impedance plot recorded in the THF solution, where  $\text{Al}_{\text{total}} = 0.5 \text{ M}$  and  $\text{AlCl}_3 : \text{LiAlH}_4 = 3$ .  $E_{\text{dc}} = -0.5 \text{ V}$ .

Table 2. Voltammetry parameters for aluminium electrodeposition (Scan rate  $0.100 \text{ V s}^{-1}$ ; all potentials  $\pm 0.02 \text{ V}$ )

Solvent	Components $\text{AlCl}_3 : \text{LiAlH}_4$	$E_1^*$ /V	$E_n^\dagger$ /V	$E'_{1/2}$ /V	$E''_{1/2}$ /V	$E'''_{1/2}$ /V	$E_{pa}$ /V	$j_{pa}$ / $\text{mA cm}^{-2}$	$Q_a$ / $\text{mC cm}^{-2}$
THF	1:3	-0.48	-0.14	-0.16	-	-	0.34	19.4	43.7
		-1.02	-0.14	-0.16	-0.48	-0.72	0.62	43	128
	1:1	-0.5	-0.13	-0.15	-0.50	-0.70	0.48	38.3	100
		-1.01	-0.13	-0.15	-0.50	-0.75	0.56	76.5	252.5
	3:1	-0.15	-0.10	-	-	-	0.12	9.5	-
		-0.50	-0.2	-0.22	-	-	0.20	68	45
		-1.0	-0.20	-0.22	-0.62	-0.94	0.60	884	308
DEE	1:1	-0.50	0.1	-	-	-	0.50	4.4	19.6
	3:1	-0.50	0.18	-	-	-	0.14	1	5.6
	7:1	-0.42	0.22	-	-	-	0.10	0.9	1.0
Xylene	2M $\text{AlBr}_3$	-0.125	-0.09	-	-	-	0.09	2.65	-

\*  $E_1$ : switching potential†  $E_n$ : nucleation potentialFig. 3. A Nyquist impedance plot recorded in the xylene solution, composed of 2M  $\text{AlBr}_3$ .  $E_{dc} = -0.6 \text{ V}$ .

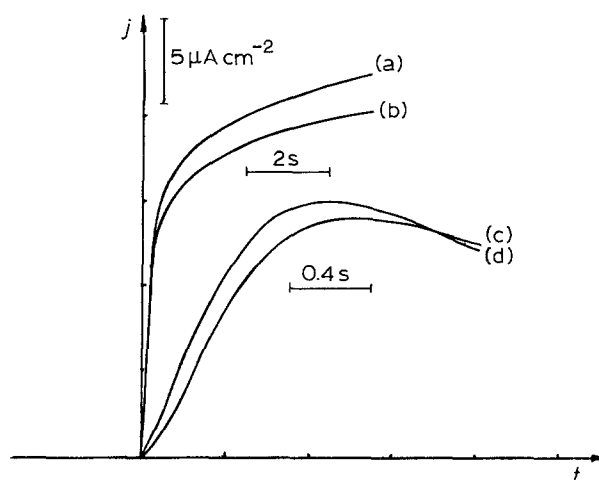
[13]. These data can distinguish between progressive and instantaneous nucleation. The plot of  $\log j_c$  against  $\log t$  gives a straight line. Its slope,  $\beta$ , provides information about the electrocrystallization process [14]. The calculated data are given in Table 4.

It was also possible to calculate, from the descending part of the  $j_c$  against  $t$  plot, diffusion coefficients  $D$  for the active species in THF. They were unexpectedly low, of the order of  $10^{-7} \text{ cm}^2 \text{ s}^{-1}$ .

Table 5 shows calculated nuclear number densities of aluminium, as a function of overpotential. The observed product  $AN_\infty$  is higher than  $N_s$  and becomes higher still as the overpotential increases. This is probably due to the onset of natural convection, which affects the diffusion zones and allows further nuclei to be formed. Finally, it appears that very fine grains can

Table 3. Kinetics data calculated from the Tafel equation

Components $\text{AlCl}_3 : \text{LiAlH}_4$	$a_c n$	$a_a n$	Solvent
1:3	0.96	0.87	THF
1:1	0.96	1.14	THF
3:1	1.44	0.90	THF
$\text{AlBr}_3$	1.08	1.80	Xylene

Fig. 4. Typical current-time curves recorded in the xylene electrolyte containing 2M  $\text{AlBr}_3$  where  $E_c$  against Al is (a)  $-0.16 \text{ V}$  and (b)  $-0.15 \text{ V}$ ; and in the THF solution containing  $\text{Al}_{\text{total}} = 0.5 \text{ M}$  and  $\text{AlCl}_3 : \text{LiAlH}_4 = 1$ , where  $E_c$  against Al is (c)  $-0.10 \text{ V}$  and (d)  $-0.14 \text{ V}$ .

be obtained if, during deposition potential does not exceed the third step in the CV curve. Preferably, it should be in the range between the first and second steps. Unfortunately no maximum was observed in the  $j-t$  curves obtained for the xylene electrolytes (Fig. 4a), so that calculation of  $N_s$  could not be done.

Figure 5 shows the plots of  $j_{Al}$  against  $\eta_{Al}$  where the

Table 4. The values of  $d \log j / d \log t$  ( $\beta$ ) and diffusion coefficients ( $D$ ) for the potentials related to various limiting currents ( $j_l$ ) for the THF solutions

$\text{AlCl}_3 : \text{LiAlH}_4$	$j_l$	$\beta$	Crystallization type	$10^7 D$ / $\text{cm}^2 \text{ s}^{-1}$ )*
1	1st	1.08	2D, progressive	0.95
	2nd	0.93	2D, instantaneous	0.52
	3rd	1.06	2D, progressive	2.03
3rd	1st	0.92	2D, instantaneous	0.88
	2nd	1.00	2D, instantaneous	0.71
	3rd	0.48	3D, instantaneous	1.82

\* Concentration of Al-complexes obtained from  $^{27}\text{Al}$  NMR data.

Table 5. Some characteristics of the aluminium nucleation process from the THF solutions\*

$E$ /mV	$10^7 AN_\infty$ /cm <sup>-2</sup> s <sup>-1</sup>	$10^7 N_s$ /cm <sup>-2</sup>	$10^7 N$ /cm <sup>-2</sup>
$AlCl_3 : LiAlH_4 = 1 \quad c = 0.376 \text{ mmol cm}^{-3}$			
-65	0.67	0.92	-
-85	2.02	1.61	-
-115	2.83	1.91	-
-125	3.01	1.97	-
-375	-	-	6.97
-405	-	-	7.19
-425	-	-	8.90
-475	-	-	12.45
-725	13.84	4.20	-
-735	15.63	4.48	-
-745	17.18	4.70	-
-755	19.26	4.98	-
$AlCl_3 : LiAlH_4 = 3 \quad c = 0.072 \text{ mmol cm}^{-3}$			
-675	-	-	125.63
-700	-	-	128.15
-725	-	-	136.44
-1000	-	-	62.07
-1025	-	-	85.41
-1050	-	-	99.33
-1075	-	-	120.29
-1150	-	-	177.41

\* Nomenclature:

- $A$  nucleation rate per active site (s<sup>-1</sup>)  
 $N_\infty$  number density of active sites (cm<sup>-2</sup>)  
 $N$  number density of growing centres (cm<sup>-2</sup>)  
 $N_s$  saturation nuclear number (cm<sup>-2</sup>)

values of  $j_{Al}$  were extracted from the impedance semi-circles. The rate of aluminium deposition from THF electrolytes increases when the overpotential also increases. The same observation applies to the xylene electrolytes provided  $\eta_{Al} < -0.5V$ . When this overpotential increases further, the rate of aluminium deposition decreases rapidly. This fact may stem from the passivation of aluminium layers during cathodic polarization. This side effect prevents the deposit from growing thicker than 20  $\mu\text{m}$ .

#### 4. Conclusions

- (i) The electrochemical deposition of aluminium from DEE and THF solutions differs only in terms of mechanism. In the case of the THF electrolytes, three types of aluminium complex discharge, while in the DEE electrolytes only one complex is involved.  
(ii) The rates of aluminium electrodeposition from the THF and xylene baths are comparable. However, on

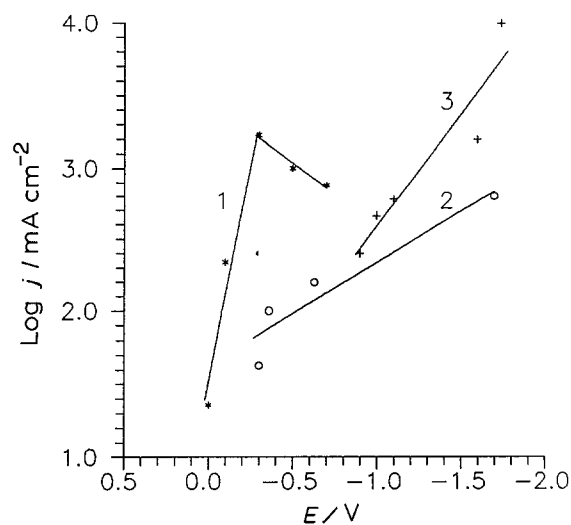


Fig. 5. A  $\log j_k - E_k$  dependence, calculated from impedance data for 2M  $AlBr_3$  solution in xylene (curve 1) and THF solutions containing  $Al_{total} = 0.5 \text{ M}$  and  $AlCl_3 : LiAlH_4 = 1$  (curve 2) and 3 (curve 3).

prolonged polarization a decrease in the deposition rate in the xylene bath is observed. The rate of aluminium deposition is much higher in the THF baths than the DEE.

(iii) Thick protective coatings of aluminium can be obtained only from THF electrolytes.

(iv) From the standpoint of the rate of aluminium electrodeposition and the deposit quality, the THF electrolyte containing  $AlCl_3$  and  $LiAlH_4$  in the ratio 1 : 1 gave superior results.

#### References

- [1] M. Galova, *Surf. Technol.* **11** (1980) 357.
- [2] V. A. Mazin, S. A. Smirnova, V. N. Titova, V. A. Kazakov, *Electrokhimiya* **25** (1989) 894.
- [3] S. Biallozor, A. Lisowska-Oleksiak, *J. Appl. Electrochem.* **20** (1990) 590.
- [4] K. Ziegler, H. Lehmkuhl, *Z. Anorg. Allg. Chem.* **283** (1956) 414.
- [5] N. Ishibashi, M. Yoshio, *Electrochim. Acta* **17** (1972) 1343.
- [6] V. A. Mazin, Dep. VINITI **N4844-B89** (1989) 22.
- [7] V. Mazin, V. A. Kazakov, S. Biallozor, *J. Electroanal. Chem.* (1993), in press.
- [8] H. Noguchi, V. A. Kazakov, H. Nakamura, M. Yoshio, *Denki Kagaku* **57** (1983) 173.
- [9] T. Agladze, 'Itogi nauki i tehniki. Seria: Korrozia i Zashchita ot Korrozii', VINITI Moscow **9** (1982) 3.
- [10] G. W. Walter, *Corros. Sci.* **26** (1986) 681.
- [11] M. Galova, D. Kladekova, L. Lux, *Surf. Technol.* **13** (1981) 315.
- [12] S. Biallozor, A. Lisowska-Oleksiak, V. A. Kazakov, V. N. Titova, N. V. Petrova, *Bull. Electrochem.* **4** (10), (1988) 884.
- [13] G. Gunawardena, G. Hills, I. Montenegro, B. Scharifker, *J. Electroanal. Chem.* **138** (1982) 225.
- [14] J. A. Harrison and H. R. Thirsk, in 'Electroanalytical Chemistry' Vol. 5 (edited by A. J. Bard) Marcel Dekker, New York (1971) p. 67.